Novel PET and Near Infrared Imaging Probes for the Specific Detection of Bacterial Infections Associated With Cardiac Devices

Kiyoko Takemiya, MD, PhD,[a] Xinghai Ning, PhD,[b] Wonewoo Seo, PhD,[c] Xiaojian Wang, PhD,[b] Rafi Mohammad, PhD,[b] Giji Joseph, MS,[a] Jane S. Titterington, MD, PhD,[a] Colleen S. Kraft, MD,[d] Jonathan A. Nye, PhD,[c] Niren Murthy, PhD,[b] Mark M. Goodman, PhD,[c] W. Robert Taylor, MD, PhD[a,e,f]

ABSTRACT

OBJECTIVES The aim of this study was to develop imaging agents to detect early stage infections in implantable cardiac devices.

BACKGROUND Bacteria ingest maltodextrins through the specific maltodextrin transporter. We developed probes conjugated with either a fluorescent dye (maltohexaose fluorescent dye probe [MDP]) or a F-18 (F18 fluoromaltohexaose) and determined their usefulness in a model of infections associated with implanted cardiac devices.

METHODS Stainless steel mock-ups of medical devices were implanted subcutaneously in rats. On post-operative day 4, animals were injected with either *Staphylococcus aureus* around the mock-ups to induce a relatively mild infection or oil of turpentine to induce noninfectious inflammation. Animals with a sterile implant were used as control subjects. On post-operative day 6, either the MDP or F18 fluoromaltohexaose was injected intravenously, and the animals were scanned with the appropriate imaging device. Additional positron emission tomography imaging studies were performed with F18-fluorodeoxyglucose as a comparison of the specificity of our probes (n = 5 to 9 per group).

RESULTS The accumulation of the MDP in the infected rats was significantly increased at 1 h after injection when compared with the control and noninfectious inflammation groups (intensity ratio 1.54 ± 0.07 vs. 1.26 ± 0.04 and 1.20 ± 0.05, respectively; $p < 0.05$) and persisted for more than 24 h. In positron emission tomography imaging, both F18 fluoromaltohexaose and F18 fluorodeoxyglucose significantly accumulated in the infected area 30 min after the injection (maximum standard uptake value ratio 4.43 ± 0.30 and 4.87 ± 0.28, respectively). In control rats, there was no accumulation of imaging probes near the device. In the noninfectious inflammation rats, no significant accumulation was observed with F18 fluoromaltohexaose, but F18 fluorodeoxyglucose accumulated in the mock-up area (maximum standard uptake value 2.53 ± 0.39 vs. 4.74 ± 0.46, respectively; $p < 0.05$).

CONCLUSIONS Our results indicate that maltohexaose-based imaging probes are potentially useful for the specific and sensitive diagnosis of infections associated with implantable cardiac devices. (J Am Coll Cardiol Img 2018;■:■-■) © 2018 by the American College of Cardiology Foundation.

Implantable cardiac devices such as prosthetic cardiac valves, pacemakers, and implantable cardioverter-defibrillators are growing in use due to increases in disease burden and expanded indications (1,2). Among these devices, the most common cardiac devices are cardiovascular implantable electronic devices (CIEDs), which include pacemakers and implantable cardioverter-defibrillators. In the United States, the number of cardiac devices implanted annually increased from approximately 350,000 to greater than 560,000 over a 5-year period (2,3). Although these medical devices provide enormous clinical benefit, there is a clear risk of device infections. The incidence of device infection after the primary pacemaker or implantable cardioverter-defibrillator implantation is approximately 0.5%, but increases by up to 10-fold after device replacement or upgrade surgery (3).

The clinical assessment of infections associated with CIEDs can be difficult due to nonspecific foreign body inflammation that may masquerade as infection (4). In addition, the diagnosis is often made after there has been extensive local infiltration or a loss of skin integrity (3,5-7). If the diagnosis of existence of bacteria in the skin pocket could be made definitively at an earlier time point in the post-operative period (particularly in patients at high risk for infection), this could potentially lead to more effective prevention and treatment of the infection that could reduce extraction of CIEDs.

We sought to develop a strategy to detect infections associated with implantable cardiac devices as well as other implantable medical devices. To this end, we identified the maltodextrin transporter for targeting bacteria because of its high uptake (V_{max} of 3.3 nmol/min/10^9 cells), and excellent specificity for bacteria (8). Also, maltodextrins are likely to be cleared from uninfected tissues due to their hydrophilic neutral composition. The maltodextrin transport system is only functional in bacteria (9). Imaging agents based on maltodextrins also have high translational potential because maltodextrins are commonly used food additives with minimal known toxicity in humans. Finally, the maltodextrin transporter only recognizes the first 2 sugars of a maltodextrin and is, thus, relatively insensitive to modifications of the remaining sugars. This potentially permits the addition of an imaging molecule tag onto a maltodextrin without significantly affecting its uptake (8-10).

With these concepts in mind, we developed 2 forms of maltohexaose-based imaging probes which have maltohexaose, a maltodextrin consisting of 6 glucose molecules, as the basic bacterial targeting unit. The first maltohexaose-based imaging probe that we developed is a maltohexaose-based near infrared fluorescent dye imaging probe, which is synthesized by conjugating the near infrared dye, IR-786 to maltohexaose (**Figure 1A**) (8). The maltohexaose fluorescent dye probe (MDP) is detectable through the skin because light in the near-infrared range is able to penetrate tissue up to several centimeters (8,11). Because generators of CIEDs are located in the subcutaneous layer, the use of MDP seems to be a plausible approach to detect pocket infections using commercially available near infrared imaging devices as a low cost and as a point of care diagnostic method. The second imaging agent that we developed is an F18-conjugated maltohexaose, F18 fluoromaltohexaose (**Figure 1B**), which incorporates ^{18}F as a radioactive tracer for positron emission tomography (PET) imaging (12). F18 fluoromaltohexaose PET imaging permits the detection of device infections in the deep organs. In this study, we demonstrate that these 2 probes are able to detect bacterial infections in a sensitive and specific manner, and that this unique approach represents a novel diagnostic strategy for the detection of existence of bacteria in an animal model of device pocket infection.

METHODS

The maltohexaose fluorescent and F18 fluoromaltohexaose probes were synthesized following previously described procedures (8,12). Briefly, the MDP was synthesized by using "click chemistry" in which maltohexaose with an azide linker was conjugated with a polyethylene glycol linker added to IR-786 (a near-infrared dye with excitation and emission wavelengths of 710/790 nm) (8). F18 fluoromaltohexaose was synthesized by 1-step nucleophilic ^{18}F fluorination of brosylate-maltohexaose (12).

MDP UPTAKE AND RETENTION BY *STAPHYLOCOCCUS AUREUS* IN VITRO. To determine if the MDP was internalized by methicillin-sensitive *Staphylococcus aureus* (MSSA) as well as the washout kinetics, 1×10^8 colony-forming units (CFU)/ml of MSSA (pulse-field gel electrophoresis typed as USA200) was cultured in Luria-Bertani (LB) broth with 20 μmol/l of MDP for 1 h at 37°C. LamB mutant *Escherichia coli* (JW3992-1), which has a mutation in the LamB protein resulting in the dysfunction of maltodextrin transportation system was used as a control. The bacteria were cultured 18 h and the plates were imaged (In-Vivo Xtreme, Bruker, Billerica, Massachusetts).

FIGURE 1 Structures of Imaging Agents

A

Maltohexaose Based Near Infrared Fluorescent Dye Probe

B
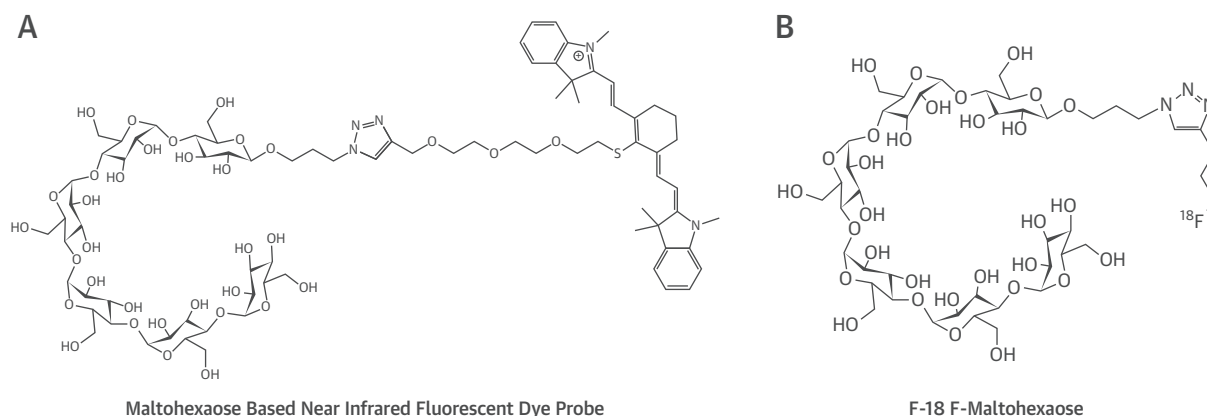
F-18 F-Maltohexaose

(A) Structural formula of maltohexaose-based near infrared fluorescent dye probe and **(B)** F18 fluoromaltohexaose.

To evaluate if the internalized fluorescent probe could be washed out from the bacteria, 20 ml of 1×10^8 CFU/ml of MSSA was cultured in LB broth with 20 μmol/l of MDP for 1 h at 37°C. The bacteria were centrifuged at 10,000×*g* for 10 min, washed 3 times with fresh LB broth, then resuspended in the same dose of fresh LB broth. The resuspended bacteria were aliquoted and incubated at 37°C. At the specified times, bacteria were centrifuged at 10,000×*g* for 10 min, washed 3 times with phosphate-buffered saline, then resuspended in phosphate-buffered saline to evaluate the concentration of MDP (n = 3 to 4 per time point).

CIED POCKET INFECTION AND NONINFECTIOUS INFLAMMATION RAT MODELS. All animal protocols were approved by the Emory University Institutional Animal Care and Use Committee. Male Sprague-Dawley rats (weighing 200 to 250 g; Jackson Laboratory, Bar Harbor, Maine) were anesthetized with 1% to 2% isoflurane, and surgical grade stainless steel mock-ups (5 × 7 × 2 mm) were implanted subcutaneously in the center of the back. On post-operative day (POD) 4, rats were divided into 3 groups: an infection group injected with 1×10^9 CFU/0.1 ml of MSSA around the mock-up (13), a noninfectious inflammation group injected with 20 μl of purified oil of turpentine (Sigma Aldrich, St. Louis, Missouri) around the mock-up as a model of sterile inflammation, and a control group that did not receive any additional treatment. The dose of MSSA was chosen to induce a relatively minor infection without rubefaction and swelling of the infected site or other systemic signs, which was intended to mimic an early stage, subclinical pocket infection. Fluorescent or PET imaging was performed on POD 6.

FLUORESCENT IMAGING. On POD 6, rats were anesthetized with isoflurane and injected with 250 μl of 1 mmol/l of the fluorescent dye probe via the tail vein (n = 6 to 9 per group). The animals were scanned with the fluorescent imaging device at the indicated times after injection of the probe and sacrificed at 24 h for histological study. Gram staining was used to evaluate for the presence of bacteria.

In some cases, cultures were obtained to quantify the level of infection. To quantify the intensity of accumulation of the probe, regions of interest (ROIs) were set around the mock-ups, and the fluorescent intensity in the ROIs and that in the entire dorsum of the animal was measured. Data were analyzed as an intensity ratio defined as the mean intensity in the mock-up area/the mean intensity in the normal skin area (arbitrary units).

PET IMAGING. On POD 6, rats (n = 5 to 6 per group) were anesthetized with isoflurane and either 250 μCi of F18 fluoromaltohexaose or 250 μCi of F18 fluorodeoxyglucose (FDG) was injected via tail vain. The rats were scanned with a micro-PET/computed tomography (Inveon Micro-PET/CT, Siemens, Munich, Germany). For quantitative analysis, transverse images 30 min after injection of F18 fluoromaltohexaose were used and the ROIs were set around the mock-up area and the normal skin area on the dorsum of the animals, contralateral to the side of the mock-ups. Quantitative assessment was made using standard uptake values (SUVs) in the ROI using the mean SUV, which is defined as [(the mean

FIGURE 2 Specific Uptake of Maltohexaose Fluorescent Dye Probe by Bacteria
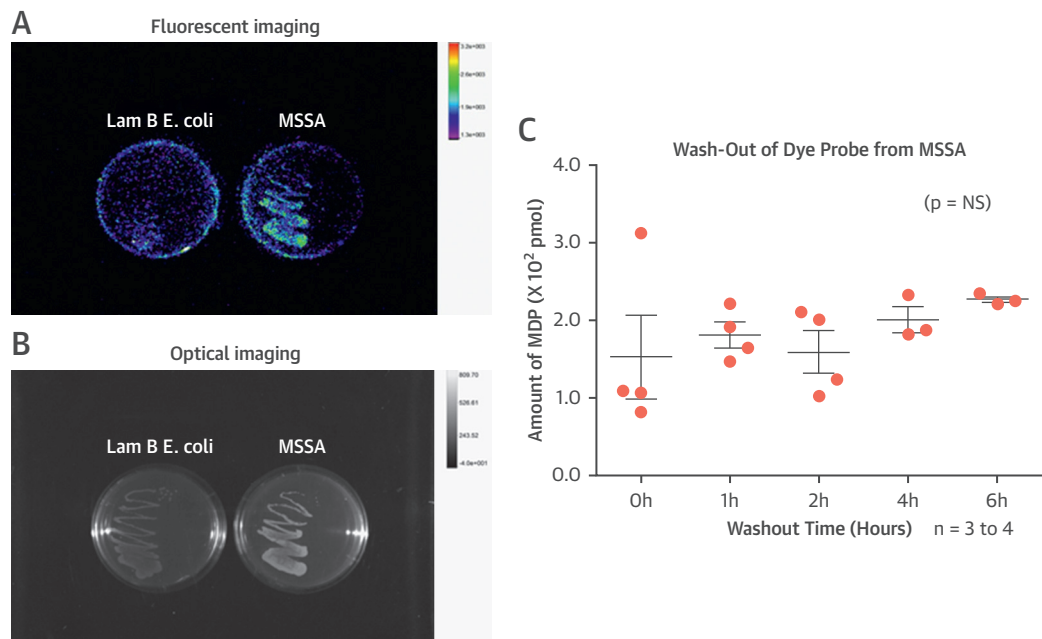
1×10^8/CFU/ml of methicillin-sensitive *Staphylococcus aureus* (MSSA) or Lam B mutant *Escherichia coli* were cultured with 20 μmol/l of maltohexaose fluorescent dye probe (MDP) for 1 h. **(A)** MSSA exhibited a clear signal, whereas Lam B mutant *Escherichia coli* had very little uptake of the dye probe. Note that there is some autofluorescence from the plastic culture dish. **(B)** Optical imaging demonstrating similar bacterial density. **(C)** For 1 h, 1×10^8/CFU/ml of MSSA was cultured with 20 μmol/l of MDP and washed. The bacterial culture was incubated Luria-Bertani broth without MDP, washed again, and the remaining MDP in bacteria quantified. In 1 h, 1×10^8/CFU of MSSA internalized $1.52 \pm 0.54 \times 10^2$ pmol of MDP, and the concentrations of fluorescent dye in MSSA showed no significant changes for up to 6 h. n = 3 to 4/time point.

radioactivity in the ROI)/(the volume of ROI)]/ [(administrated radioactivity)/(body weight)] and maximum SUV defined as (the highest pixel value in the ROI)/[(administrated radioactivity)/(body weight)]. Data were analyzed using the ratios of the SUV to account for differences in body weight as previously described (14,15).
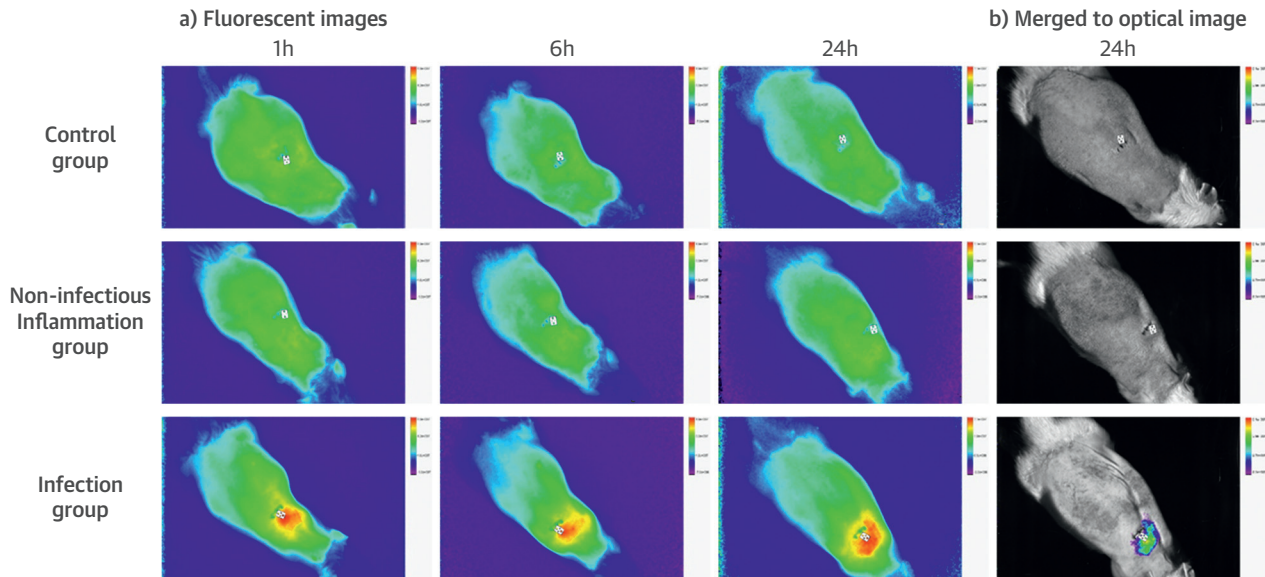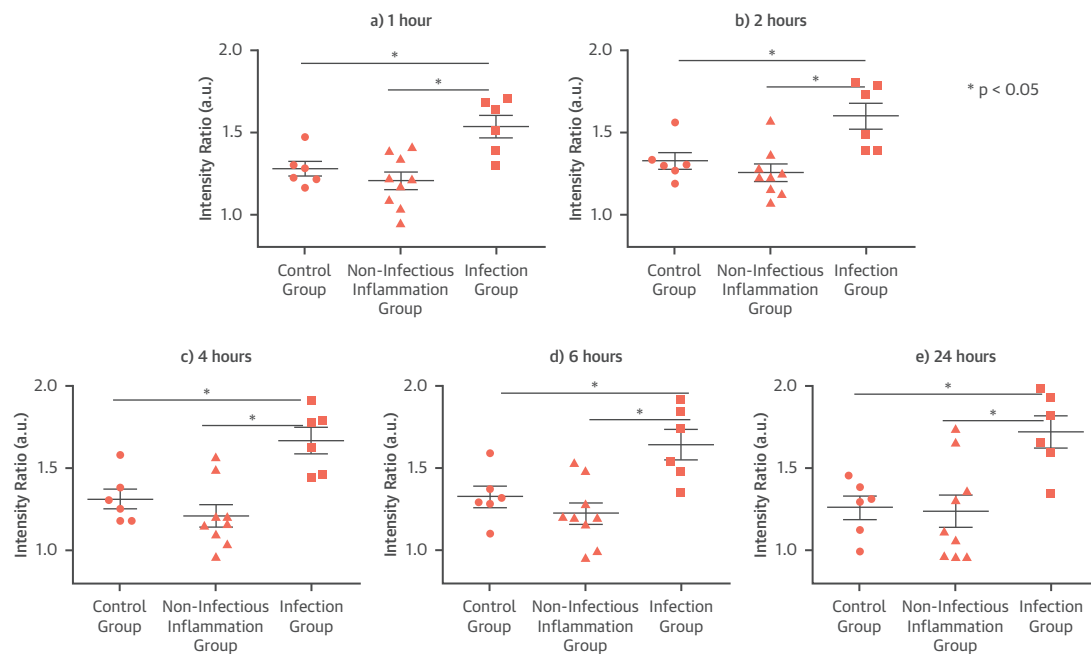
BIOFILM MODEL. Stainless steel mock-ups were implanted subcutaneously in the center of the back 10 to 14 days before inoculation. At this time point, fibrous pockets were fully formed around the mock-ups and MSSA colonies consisting of bacteria embedded in matrix cultured on LB agar plates placed on the mock-ups through a 24-G plastic catheter. In this model, the bacteria are embedded in acellular matrix which mimics a biofilm on an implanted generator and do not spread into surrounding tissues. Two days after inoculation, the rats were imaged as described for fluorescent (n = 7) or PET/computed tomography imaging (n = 3).

BIODISTRIBUTION OF MDP. Healthy rats were injected with 250 μl of 1 mmol/l dye probe via the tail vein and kept in metabolic cages to collect the feces and urine for 24 h (n = 4). Blood and tissue were harvested using standard techniques. The amount of probe in the organs was calculated based on the concentrations in the sample and quantified as the percent of injected dye.

STATISTICAL ANALYSIS. Analysis was performed with Prism statistical software. For comparison of 2 groups, the Student *t* test was used, and 1-way analysis of variance with Tukey's multiple comparison test was used for multigroup comparison. All data are shown as mean ± SE and p < 0.05 was regarded as significant.

RESULTS

MDP IS EFFECTIVELY TAKEN UP AND RETAINED BY *S AUREUS* IN VITRO. MSSA internalized the MDP after 1 h, and the probe remained internalized in

ARTICLE IN PRESS

JACC: CARDIOVASCULAR IMAGING, VOL. ■, NO. ■, 2018   Takemiya *et al.*   5
■ 2018: ■ - ■   New Imaging Probes to Detect Device Infection

FIGURE 3 Fluorescent Imaging with Maltohexaose Fluorescent Dye Probe In Vivo

(A) Robust accumulation of maltohexaose fluorescent dye probe (MDP) was seen around the mock-up in the infection group as soon as 1 h after the injection of the dye probe, although no significant accumulation was observed in the noninfectious inflammation group and in the control group. (B) The corrected intensity ratios in the infection group were significantly increased compared with those in the noninfectious inflammation group and in the control group at all time points. n = 6 to 9 per group. *p < 0.05.

FIGURE 4   Demonstration of the Presence of Bacteria in the Infected Mock-Ups
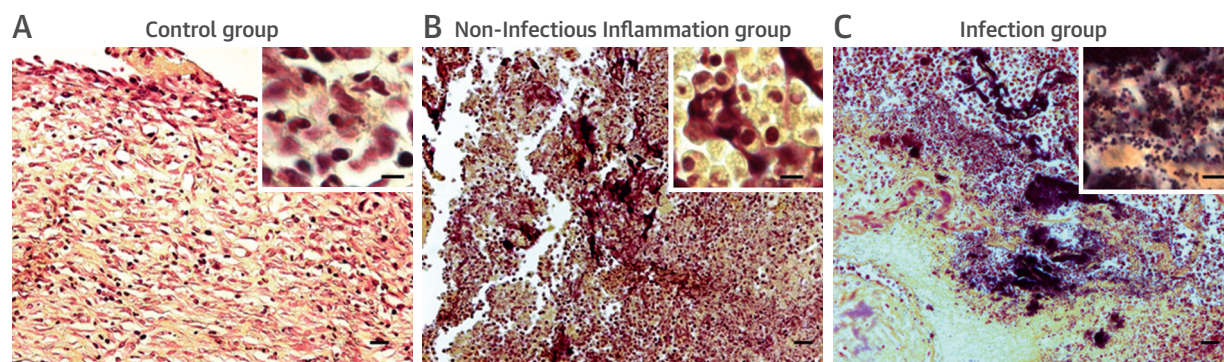
Skin samples around the mock-ups demonstrated an inflammatory response that was seen in all groups **(A to C)** but was most intense in the inflammation **(B)** and infection groups **(C)**. Note that, as expected, gram positive cocci were seen only in the infection group **(C)**. Original magnification 20X, bars, 20 μm. Original magnification in the inset 1X; bars 5 μm.

MSSA for at least 6 h (**Figure 2**). In contrast, LamB mutant bacteria, which lack the maltodextrin transporter, internalized almost no dye probe as indicated by very little fluorescent signal (**Figure 2**). In the quantitative analysis (**Figure 2C**), 1×10^8 CFU of MSSA internalized $1.52 \pm 0.54 \times 10^2$ pmol of MDP in 1 h. Importantly, the concentrations of fluorescent dye in MSSA showed no significant decrease in intensity over 24 h, indicating retention of the imaging agent. These data demonstrate that the MDP is internalized by MSSA very specifically through the maltodextrin transport system and is a stable fluorescent imaging agent for bacteria.

FLUORESCENT IMAGING. The potential usefulness of MDP to detect bacterial infection with high sensitivity and specificity was evaluated using a rat model. Rats injected with bacteria exhibited no obvious signs of infection at the site of the device implantation. As shown in **Figure 3A**, the MDP accumulated around the mock-up area in the infection group as soon as 1 h after injection of the dye probe and persisted for at least 24 h. Conversely, no significant accumulation of the dye probe was found in either the control group or in the noninfectious inflammation group. In the quantitative analysis (**Figure 3B**), the intensity ratio, which indicates the relative accumulation of probe in the infected mock-up area compared with that in the normal skin area was 1.54 ± 0.07 at 1 h after the injection of maltohexaose dye probe, and was significantly higher than the noninfectious inflammation group and the control group (1.20 ± 0.05 and 1.28 ± 0.04, respectively; $p < 0.05$). No significant difference was found between the noninfectious inflammation group and the control group, demonstrating the

specificity of the MDP to detect infection as opposed to inflammation. These data indicated that the MDP accumulated in the site of infection in a highly specific manner with an excellent signal-to-noise ratio. Conversely, in the noninfectious inflammation model, there was no significant accumulation of the dye probe in the mock-up area.

Histological analysis of the tissue adjacent to the site of implantation of the mock-ups confirmed the presence of bacteria in the infected group as well as sterility in the control and the noninfectious inflammation groups (**Figure 4**). At the time of imaging, the total bacterial burden was 2.9×10^8 CFU (n = 4). There was an intense inflammatory response in turpentine treated animals (**Figure 4**). These same animals demonstrated no significant uptake of maltohexaose dye probe.

PET IMAGING. We also developed a PET imaging agent using the same targeting strategy to image infections in deeper tissues. We examined the sensitivity and the specificity of F18 fluoromaltohexaose and compared it with FDG. The averages of mean SUV of the normal skin area of all animals were 0.205 ± 0.028 in F18 fluoromaltohexaose PET imaging and 0.835 ± 0.04048 in FDG PET imaging, indicating the low metabolism and the rapid clearance of F18 fluoromaltohexaose in animals. As shown in **Figure 5**, both F18 fluoromaltohexaose and FDG demonstrated significant accumulation around the mock-ups in the infection group (ratio of the mean SUV 2.87 ± 0.206 and 2.86 ± 0.26, respectively; ratio of the maximum SUV 4.43 ± 0.30 and 4.87 ± 0.28, respectively), and neither showed any significant accumulation of tracer in around the mock-ups in the control group.

FIGURE 5 **FMH and FDG PET Imaging In Vivo**

A FMH PET Imaging on the model rats
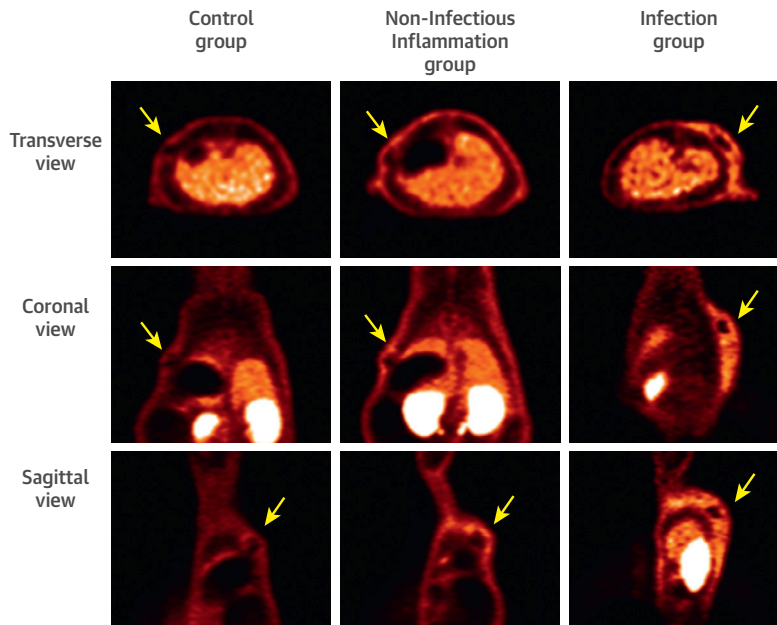
B FDG PET Imaging on the model rats
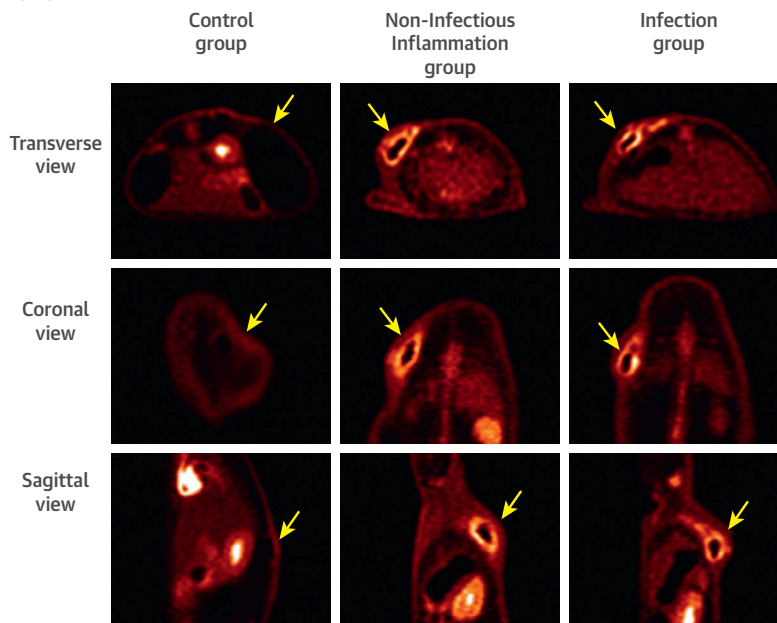
(A) F18 fluoromaltohexaose (FMH) accumulation was clearly observed in the infection group with very low accumulation in the control group and in the noninfectious inflammation group. Conversely, with positron emission tomography (PET) imaging with F18 fluorodeoxyglucose (FDG) **(B)**, the accumulation of radioactivity was observed in the infection group as well as in the noninfectious inflammation group. **Yellow arrows** indicate the locations of the mock-ups. For FMH PET imaging, the infection group had a significant increase in both ratio of the maximum standard uptake value (SUV_{max}) and ratio of the mean standard uptake value ($SUVR_{mean}$) when compared with both the control group and the noninfectious inflammation group. With FDG PET imaging, the infection group and the noninfectious inflammation group had a similar, significant increase in both SUV_{max} and $SUVR_{mean}$ when compared with the control group demonstrating a lack of specificity **(C)**. n = 5 to 6 per group. *p < 0.05.
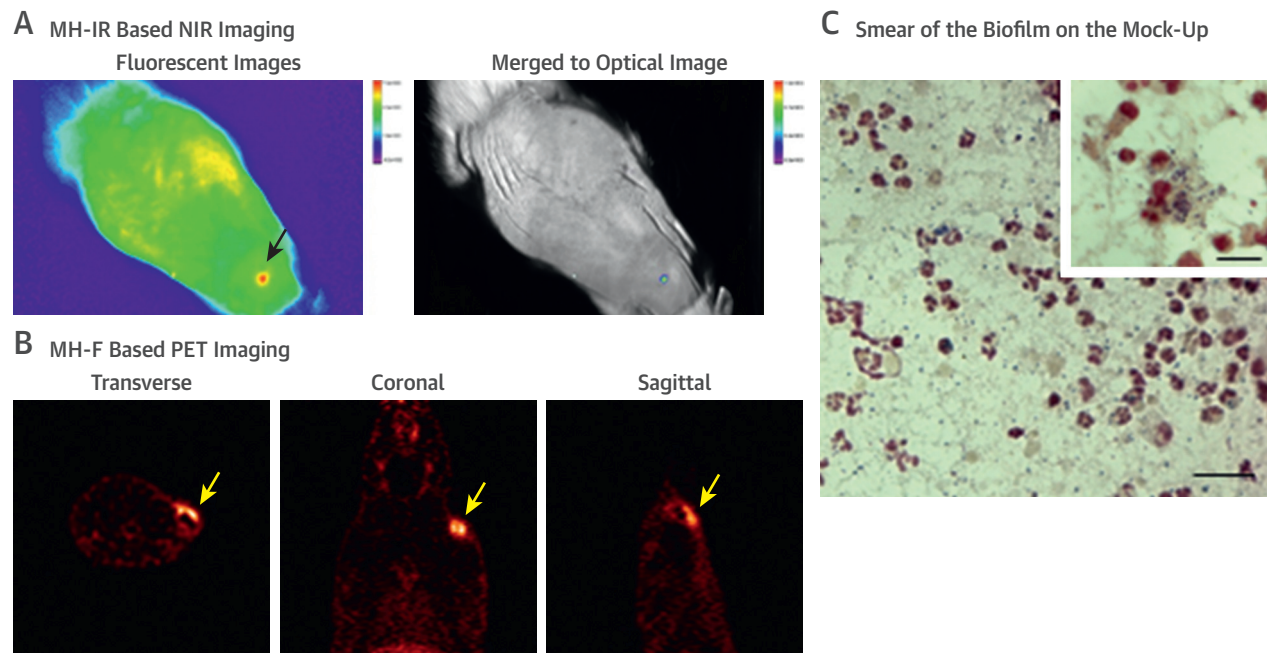
FIGURE 5 Continued
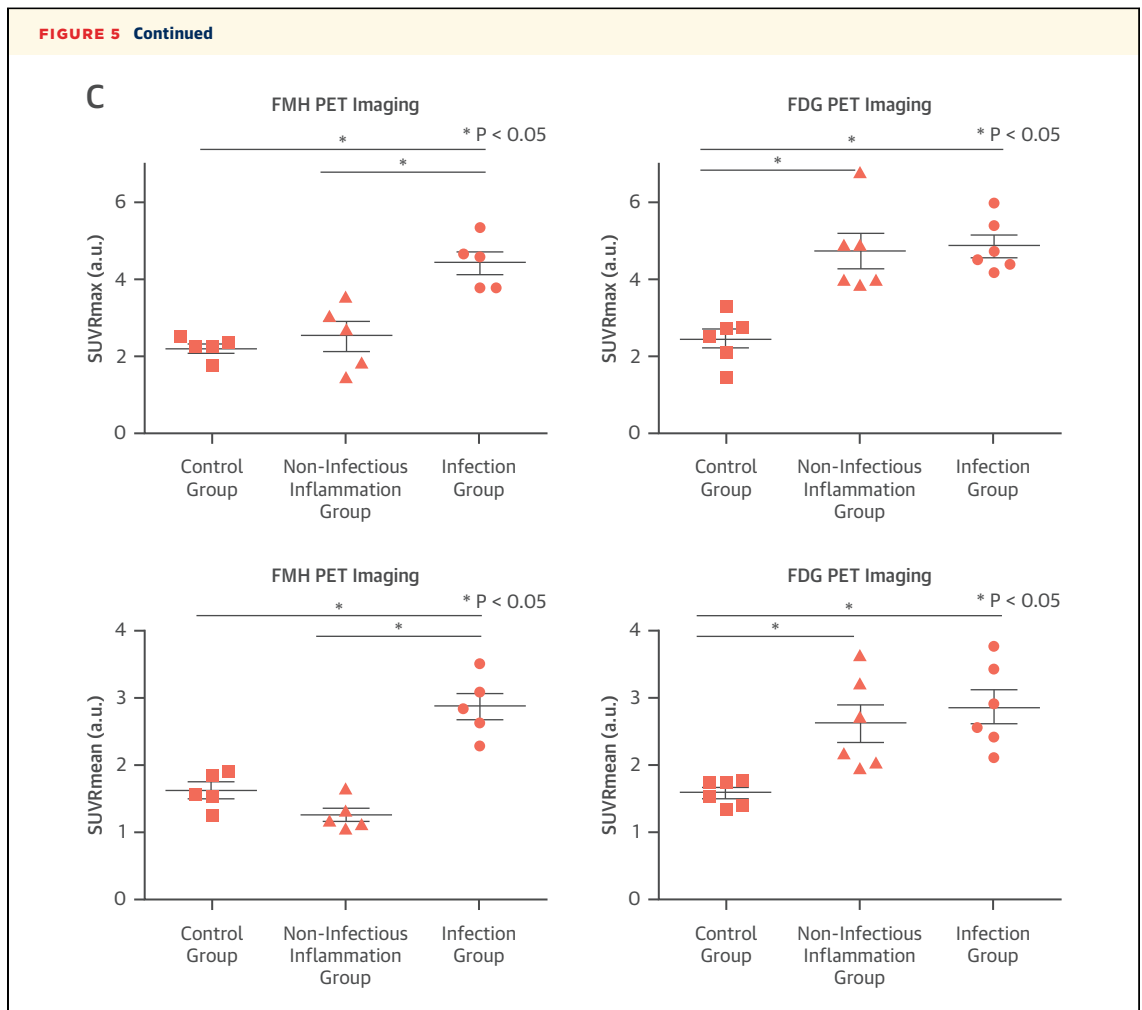
However, in the noninfectious inflammation group, F18 fluoromaltohexaose showed no significant accumulation around the mock-ups, whereas FDG accumulated around the mock-ups (ratio of the mean SUV, 1.26 ± 0.11 and 2.62 ± 0.28, respectively; ratio of the maximum SUV, 2.53 ± 0.39 and 4.74 ± 0.46, respectively). The findings with FDG are consistent with common clinical observations of poor specificity of FDG in this setting due to the lack of ability to discern between inflammation and infection.

DETECTION OF BACTERIA IN A BIOFILM. We evaluated the ability of our maltodextrin-based imaging probes to detect bacteria embedded in a biofilm. The amount of MSSA delivered to the mockups ranged from 7.3×10^6 to 6.6×10^7 CFU (mean $2.3 \pm 1.2 \times 10^7$ CFU) as the precise amount of bacteria implanted could not be pre-determined. At the time of imaging, the total bacterial burden had decreased to $6.3 \pm 4.6 \times 10^5$ CFU. On histological evaluation, no invasion of bacteria outside of the fibrous pocket was found,

but in the smear made with the tissue attached to the mock-ups, scattered Gram-positive cocci with neutrophils and macrophages were observed, demonstrating the existence of a biofilm similar to that seen in the clinical setting. Despite this modest bacterial burden and the presence of a biofilm, both the maltohexaose fluorescent dye and the F18 fluoromaltohexaose PET imaging probes were able to detect bacteria in this in vivo model of a biofilm (Figure 6).

BIODISTRIBUTION OF THE MDP. The distribution of MDP was evaluated in the healthy rats. Twenty-four hours after injection of the maltohexaose dye probe, $45.5 \pm 6.7\%$ of the injected probe was excreted into the feces, and only $0.4 \pm 0.1\%$ was excreted into the urine. The MDP was primarily found in the liver and MDP in the kidneys was low ($3.8 \pm 0.7\%$ and $1.1 \pm 0.2\%$, respectively). The concentration of MDP in the intestine was $0.52 \ \mu mol/l$ ($1.2 \pm 0.5\%$ of injected probe). Other organs, such as the spleen, heart, and

ARTICLE IN PRESS

JACC: CARDIOVASCULAR IMAGING, VOL. ■, NO. ■, 2018
■ 2018:■ - ■

Takemiya et al.
New Imaging Probes to Detect Device Infection

9

FIGURE 6 Detection of Bacteria in a Biofilm on Implanted Mock-Up Devices

A MH-IR Based NIR Imaging

Fluorescent Images   Merged to Optical Image

C Smear of the Biofilm on the Mock-Up

B MH-F Based PET Imaging

Transverse   Coronal   Sagittal

Rats were implanted with the mock-up devices, and a small amount of biofilm forming MSSA was inoculated on the implanted mock-up devices as a biofilm model. Two days after inoculation, the rats were injected with the MDP or FMH via the tail vein. Both the MDP **(A)** and FMH **(B)** accumulated at the site of the infected mock-up device. **Arrows** indicate locations of the mock-ups. Abbreviations as in **Figures 2 and 5**.

---

lungs, contained <1% of injected probe. Other tissue, such as the muscles and the skin, contained a small amount of MDP below the level of quantitative detection. Because of the short half-life of F18, we did not evaluate the distribution of F18 fluoromaltohexaose 24 h after injection. However, significant accumulation of the tracer was found in the bladder, indicating that F18 fluoromaltohexaose is excreted primarily into the urine at these early time points.

DISCUSSION

In this study, we present robust preclinical data demonstrating the usefulness of targeting the maltodextrin transporter to identify the presence of bacteria in a very sensitive and specific manner. We demonstrated that both the maltohexaose fluorescent dye and F18 fluoromaltohexaose probes were able to detect very early stage bacterial infections in a model of subclinical infection of device pocket infection in rats.

The diagnosis of pocket infection related to cardiac devices is an important clinical problem in medicine

today. Due to the expanding use of implantable medical devices, the large number of immunocompromised patients, an aging population, and the emergence of drug-resistant bacteria, the number of patients with infected medical devices continues to increase (1,2,16). The number of hospital admissions for CIED infections has increased 3-fold over an 8-year period, paralleling a similar increase in the number of device infections. Importantly, pocket infections are associated with at least a doubling of mortality (17). The incremental cost associated with infection of an implantable electronic cardiac device is estimated to be in excess of $50,000 per patient (18).

In our experiments, we intentionally performed the in vivo studies using a very mild degree of infection to mimic a preclinical infection. The infected animals exhibited no overt signs of infection at the site of the infected mock-ups and had no systemic signs of infection. We undertook this strategy to test the ability of maltohexaose based imaging probes to detect bacteria at a stage of infection that is clinically challenging. This finding raises the possibility that, in select patients with early stage infection, there exists

the possibility to effectively treat the infection with antibiotics without the need to extract the device. In addition, our approach to bacterial imaging could also be used to monitor the efficacy of antibiotic therapy. The impact of this approach on morbidity and mortality as well as the costs associated with infected medical devices could be very significant.

Our studies demonstrated that the MDP was internalized by MSSA and that the accumulated fluorescent MDP remained in MSSA without a loss of the fluorescent activity. MSSA was used in this study because it is one of the most common causes of the pocket infections. However, the maltodextrin transport system exists universally in all bacteria, and we have previously shown that a maltodextrin conjugated dye probe is internalized by many species of bacteria (8). These characteristics make a MDP potentially very useful in many clinical applications because of the persistence of the signal and the ability to detect a wide range of bacteria.

We also showed that MDP detected subclinical bacterial pocket infections in rats with high sensitivity and high specificity using near infrared fluorescent imaging. Optical imaging strategies in general are limited by the ability to detect the probes in deeper tissues. However, the use of near infrared dyes mitigates this limitation to some degree because detection up to several centimeters is possible with commercially available equipment (19). In the specific case of CIEDs, there is the advantage that the generator is generally located in the subcutaneous space near the surface of the skin. Although the leads of CIEDs are significantly deeper in the body, and infection at these sites would not be readily detected by surface optical imaging strategies, the majority of CIED infections involve the generator and pocket (3). Even though the sensitivity of MDP is very likely less than that of F18 fluoromaltohexaose, the MDP still has sufficient sensitivity to detect the existence of very small amounts of bacteria. Furthermore, near infrared imaging is less expensive than PET imaging and could be used at the bedside without the need for extremely expensive imaging equipment. This advantage may be particularly useful in those patients at increased risk for infections associated with CIEDs (e.g., patients with diabetes, patients on hemodialysis).

We also developed a PET imaging-based strategy using F18 fluoromaltohexaose that is similarly very sensitive and specific for detecting the existence of bacteria. This imaging agent is superior to FDG due to its ability to distinguish bacterial infection from sterile inflammation in vivo. Although PET imaging requires dedicated facilities and higher cost than fluorescent imaging, the improved sensitivity of PET imaging may ultimately prove to be very beneficial.

The use of imaging agents to effectively detect localized bacterial infections has been the goal of several previous investigations. Sarrazin et al. (4) originally reported that FDG PET imaging was effective in the diagnoses of skin pocket infection with approximately 90% of specificity. An important difference between their study and ours is that we were able to discern between intense sterile inflammation and true infection with the maltohexaose-based probes. For both the fluorescent and PET imaging probes, no significant uptake was observed in the turpentine model of sterile inflammation. This finding was in contrast with the positive uptake observed with FDG imaging of sterile inflammation. These results support the main thesis of our study that maltohexaose-based imaging probes are specifically internalized by bacteria and that, because of the increased specificity and sensitivity, these novel imaging agents may prove to be a valuable tool to image bacterial infections associated with implantable cardiac devices.

Recently, Zhang et al. (2) studied the ability of radioactively labeled fialuridine, [^{124}I]FIAU (a nucleoside analog which is a substrate for bacterial thymidine kinase), to detect bacterial infections associated with prosthetic joints. Despite promising preclinical studies, the human studies failed to demonstrate efficacy of this approach (20). A major contributor to the failure of their studies was the nonspecific muscle uptake of FIAU (20). In contrast with [^{124}I]FIAU, the advantage of F18 fluoromaltohexaose is that there is very likely markedly lower nonspecific uptake by mammalian tissues.

Using the same approach of targeting the maltodextrin transporter as we initially described (12), Gowrishankar et al. (21) reported that F18 labeled fluoromaltose was able to detect bacterial infections caused by *E. coli* in a mouse thigh abscess model. Subsequent work by the same group reported on the development of a related compound, 18F-fluoromaltotriose which possesses improved urinary clearance when compared with their original fluoromaltose imaging agent (22). A comparison of imaging efficacy was not carried out. These studies support the overall concept of targeting the maltodextrin transporter and raise the possibility that these or other modifications may impact the biodistribution and potentially the efficacy.

STUDY LIMITATIONS. The potential application of these imaging probes extends beyond the ability to diagnose device pocket infections. Although there

may be issues with gating and subsequent spatial resolution of cardiac structures, these agents could potentially be used to diagnose endocarditis of native or prosthetic heart valves as well as infections associated with left ventricular assist devices and other cardiovascular implants. Maltodextrin-based imaging agents may be useful in other clinical settings as well, including infections associated with orthopedic implants, identifying the source of bacteremia, diagnosing bacterial infections of the lungs, and so on. Moreover, it is suggested that our strategy of specific molecular delivery to bacteria with maltohexaose could be a platform for targeting therapeutics to bacteria or could potentially be expanded as a "theranostic" to image bacteria and simultaneously directly target antibacterial agents.

CONCLUSIONS

Targeting the maltodextrin transporter is an effective strategy for delivering imaging agents to bacteria to diagnose and localize bacterial infections. We developed both fluorescent and PET imaging agents that are potentially useful for the specific diagnosis of bacterial infections associated with implanted cardiac devices. This strategy has the potential to positively impact the morbidity and mortality as well as the health care costs associated with infections of implanted medical devices. Moreover, our study suggests that maltodextrins can be molecular vectors specific for bacteria with broader applications for the diagnosis and treatment of bacterial infections.

ADDRESS FOR CORRESPONDENCE: Dr. W. Robert Taylor, Department of Medicine, Division of Cardiology, Emory University School of Medicine, 101 Woodruff Circle, Suite 319 WMB, Atlanta, Georgia 30322. E-mail: wtaylor@emory.edu. OR Dr. Niren Murthy, Department of Bioengineering, University of California Berkeley, 284 Hearst Memorial Mining Building, Berkeley, California 94720. E-mail: nmurthy@berkeley.edu. OR Dr. Mark Goodman, Center for Systems Imaging, Department of Radiology and Imaging Sciences, Emory University, 1841 Clifton Rd, NE, WWHC209, Atlanta, Georgia 30329. E-mail: mgoodma@emory.edu.

PERSPECTIVES

COMPETENCY IN MEDICAL KNOWLEDGE: The accurate diagnosis of bacterial infections associated with implanted medical devices remains a significant medical issue that continues to grow as our population ages and the indications for these devices broaden. Currently available imaging modalities suffer from insufficient diagnostic accuracy and additional approaches are needed.

TRANSLATIONAL OUTLOOK: Novel approaches are needed to identify infections associated with medical devices as current methods of imaging white blood cells have inherent limitations. The maltodextrin transporter is a unique bacterial target that opens up the possibility of developing a family of highly specific imaging agents for bacteria.

REFERENCES

1. Olsen NT, De Backer O, Thyregod HG, et al. Prosthetic valve endocarditis after transcatheter aortic valve implantation. Circ Cardiovasc Interv 2015;8:e001939.

2. Greenspon AJ, Patel JD, Lau E, et al. 16-year trends in the infection burden for pacemakers and implantable cardioverter-defibrillators in the United States 1993 to 2008. J Am Coll Cardiol 2011;58:1001–6.

3. Tarakji KG, Wilkoff BL. Management of cardiac implantable electronic device infections: the challenges of understanding the scope of the problem and its associated mortality. Expert Rev Cardiovasc Ther 2013;11:607–16.

4. Sarrazin JF, Philippon F, Tessier M, et al. Usefulness of fluorine-18 positron emission tomography/computed tomography for identification of cardiovascular implantable electronic device infections. J Am Coll Cardiol 2012;59:1616–25.

5. Nataloni M, Pergolini M, Rescigno G, Mocchegiani R. Prosthetic valve endocarditis. J Cardiovasc Med 2010;11:869–83.

6. Habib G, Hoen B, Tornos P, et al. Guidelines on the prevention, diagnosis, and treatment of infective endocarditis (new version 2009): the Task Force on the Prevention, Diagnosis, and Treatment of Infective Endocarditis of the European Society of Cardiology (ESC). Eur Heart J 2009;30:2369–413.

7. Chen W, Kim J, Molchanova-Cook OP, Dilsizian V. The potential of FDG PET/CT for early diagnosis of cardiac device and prosthetic valve infection before morphologic damages ensue. Curr Cardiol Rep 2014;16:459.

8. Ning X, Lee S, Wang Z, et al. Maltodextrin-based imaging probes detect bacteria in vivo with high sensitivity and specificity. Nat Mater 2011;10:602–7.

9. Gopal S, Berg D, Hagen N, et al. Maltose and maltodextrin utilization by Listeria monocytogenes

depend on an inducible ABC transporter which is repressed by glucose. PloS One 2010;5: e10349.

10. Dahl MK, Manson MD. Interspecific reconstitution of maltose transport and chemotaxis in Escherichia coli with maltose-binding protein from various enteric bacteria. J Bacteriol 1985;164: 1057–63.

11. Hilderbrand SA, Weissleder R. Near-infrared fluorescence: application to in vivo molecular imaging. Curr Opin Chem Biol 2010;14:71–9.

12. Ning X, Seo W, Lee S, et al. PET imaging of bacterial infections with fluorine-18-labeled maltohexaose. Angew Chem Int Ed Engl 2014;53: 14096–101.

13. Tseng CW, Sanchez-Martinez M, Arruda A, Liu GY. Subcutaneous infection of methicillin resistant Staphylococcus aureus (MRSA). J Vis Exp 2011;9:48.

14. Boellaard R, Delgado-Bolton R, Oyen WJ, et al. FDG PET/CT: EANM procedure guidelines for tumour imaging: version 2.0. Eur J Nucl Med Mol Imaging 2015;42:328–54.

15. Johnsrud K, Skagen K, Seierstad T, Skjelland M, Russell D, Revheim ME. (18)F-FDG PET/CT for the quantification of inflammation in large carotid artery plaques. J Nucl Cardiol 2017 Dec 5 [E-pub ahead of print].

16. Tarakji KG, Chan EJ, Cantillon DJ, et al. Cardiac implantable electronic device infections: presentation, management, and patient outcomes. Heart Rhythm 2010;7:1043–7.

17. Baddour LM, Epstein AE, Erickson CC, et al. Update on cardiovascular implantable electronic device infections and their management: a scientific statement from the American Heart Association. Circulation 2010;121:458–77.

18. Sohail MR, Henrikson CA, Braid-Forbes MJ, Forbes KF, Lerner DJ. Mortality and cost associated with cardiovascular implantable electronic device infections. Arch Intern Med 2011;171: 1821–8.

19. Kitai T, Inomoto T, Miwa M, Shikayama T. Fluorescence navigation with indocyanine green for detecting sentinel lymph nodes in breast cancer. Breast Cancer 2005;12:211–5.

20. Zhang XM, Zhang HH, McLeroth P, et al. [(124)I]FIAU: human dosimetry and infection imaging in patients with suspected prosthetic joint infection. Nucl Med Biol 2016;43:273–9.

21. Gowrishankar G, Namavari M, Jouannot EB, et al. Investigation of 6-[(1)(8)F]-fluoromaltose as a novel PET tracer for imaging bacterial infection. PloS One 2014;9:e107951.

22. Gowrishankar G, Hardy J, Wardak M, et al. Specific imaging of bacterial infection using 6"-(18)F-fluoromaltotriose: a second-generation PET tracer targeting the maltodextrin transporter in bacteria. J Nucl Med 2017;58:1679–84.

KEY WORDS bacterial imaging, medical device infections, optical imaging, PET